



Contents lists available at SciVerse ScienceDirect

Bioorganic & Medicinal Chemistry

journal homepage: www.elsevier.com/locate/bmcReduced glutathione-resisting ^{19}F NMR sensors for detecting HNO

Narufumi Kitamura, Tatsuhiro Hiraoka, Kazuo Tanaka, Yoshiki Chujo *

Department of Polymer Chemistry, Graduate School of Engineering, Kyoto University, Katsura, Nishikyo-ku, Kyoto 615-8510, Japan

ARTICLE INFO

Article history:

Received 17 April 2012

Revised 6 June 2012

Accepted 6 June 2012

Available online 15 June 2012

Keywords:

HNO

 ^{19}F NMR probe

POSS

Paramagnetic relaxation enhancement

ABSTRACT

The ^{19}F NMR probes for the HNO detection are reported. We synthesized the probe molecules with the paramagnetic Cu(II) complex and fluorine atoms using a cubic silsesquioxane. By using the magnetism changes of the Cu(II) to Cu(I) in the complex by the reduction with HNO, the ^{19}F NMR signal intensities of the probe increased. Noteworthy, our probes have superior resistance to reduced glutathione which is the major intracellular molecule to maintain the reductive environment and the competitor in the reduction of Cu(II) against HNO.

© 2012 Elsevier Ltd. All rights reserved.

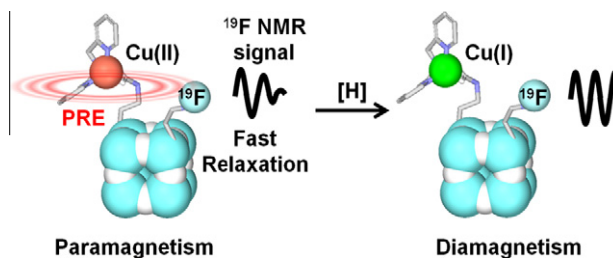
1. Introduction

Nitroxyl (HNO), the one-electron reduced and protonated analogue of NO, has attracted much attention because of unique and potentially significant biological activities, and further investigations have been vigorously executed for understanding their behaviors in details.¹ In recent years, Lippard et al. and following other groups presented the HNO-selective fluorescence probes using the Cu complex of bis(2-pyridylmethyl)amino-2-ethanoic acid (PMEA) and chromophore conjugations and successfully detected the generation of HNO in the cells.^{2,3} By reducing Cu(II) to Cu(I) by HNO, the alteration of the quenching ability of the Cu complex was induced. Thereby, the probe showed the different optical properties. On the other hand, it was demonstrated that the probes showed slight changes in the presence of other nitrogen oxides such as NO, NO₂ and ONOO[−].² Thus, the HNO detection can be achieved utilizing these optical probes. For further understanding the biological significance of HNO, there is another issue to be overcome. The crucial problem in the HNO detection based on the Cu reduction of the PMEA complexes is caused by the existence of the much larger amount of reduced glutathione (GSH)⁴, which is the buffering material for maintaining the intracellular reductive environments. In particular, GSH coordinates and reduces the Cu(II) ion in the complex.⁵ Thus, to extend the applicability of the HNO probes, the new materials which can distinguish HNO in the presence of GSH should be strongly required.

For monitoring the behaviors of HNO in vital organisms, a non-invasive detection modality is suitable. We have focused on the ^{19}F

NMR spectroscopy as a main modality to monitor the biological events and quantifying the functions of biomolecules.⁶ In particular, we established to assemble the various functional molecules involving fluorine atoms onto the water-soluble biocompatible scaffold using octaamino polyhedral oligomeric silsesquioxane (POSS) derivatives⁷ according to preprogramed designs and regulate the NMR signals corresponded to the recognition of the target biomolecules or functions. Moreover, other stimuli-responsive fluorine-containing materials have been applied as ^{19}F MRI contrast agents for monitoring the biological molecules and events such as gene repression,⁸ protein existence,⁹ enzymatic activity,¹⁰ environmental alteration,¹¹ cell viability,¹² and biological reactions.¹³ Thus, the ^{19}F NMR probes which can detect HNO are promised to be feasible for clarifying the behaviors of HNO in details.

Herein, we describe the ^{19}F NMR probes for detecting HNO. The water-soluble multi-component probes involving the Cu–PMEA complex as the signal switch for ^{19}F NMR were synthesized. Before the detection for HNO, the probe shows slight NMR signals because of the paramagnetic relaxation enhancement (PRE)^{13,14} by



Scheme 1. Signal regulation of ^{19}F NMR by changing the magnetism with the reduction of the metal complex in the probe.

* Corresponding author. Tel.: +81 75 383 2604; fax: +81 75 383 2605.

E-mail address: chujo@chujo.synchem.kyoto-u.ac.jp (Y. Chujo).

the Cu(II) ion (Scheme 1). By adding the HNO generator in the solution, the Cu(II) ion in the PMEAs complex should be reduced, resulting in the production of Cu(I) which shows diamagnetism. Thereby, the significant increase of the peak width in ^{19}F NMR was observed from the probes with the same pulse sequence and NMR parameters. Remarkably, the ^{19}F NMR signals from our probe were less influenced by adding GSH. This means our probe molecule has resistant to GSH. This is, to the best of our knowledge, the first example not only to offer the HNO probe with ^{19}F NMR spectroscopy but also to accomplish the detection with the durability toward the GSH reduction.

2. Experimental section

2.1. General

^1H NMR and ^{13}C NMR spectra were measured with a JEOL EX-400 spectrometer operating at 400 MHz for ^1H and 100 MHz for ^{13}C , respectively. ^{19}F and ^{29}Si NMR spectra were measured with a JEOL JNM-A400 spectrometer operating at 370 MHz for ^{19}F and 80 MHz for ^{29}Si , respectively. Coupling constants (J value) are reported in Hertz. The chemical shifts in ^{19}F NMR are expressed in ppm downfield from trifluoroacetic acid as an external reference. Masses were determined with a MALDI-TOF mass spectroscopy (acceleration voltage 21 kV, negative mode) with 2,5-dihydroxybenzoic acid (DHB) as a matrix. Angeli's salt was purchased from Aldrich (USA) and used without further purification. Recyclable preparative high-performance liquid chromatography (HPLC) was performed on a Model LC918R (Japan Analytical Industry Co. Ltd, Tokyo, Japan) equipped with JAIGEL-1H and 2H columns (GPC) in chloroform as an eluent. 4-(4,6-Dimethoxy-1,3,5-triazin-2-yl)-4-methylmorpholinium chloride (DMT-MM) was purchased from Wako Pure Chemical Industries, Ltd (Tokyo, Japan).

2.2. Compound 1¹⁵

The solution containing 2,2'-dipicorylamine (2.0 g, 10 mmol), K_2CO_3 (1.44 g, 10 mmol), and *tert*-butyl bromoacetate in dry DMF (10 mL) was stirred at room temperature for 24 h. After the filtration, the solvent in the filtrate was removed in vacuo. The residue was dissolved in dichloromethane and washed with satd NaHCO_3 aq four times and brine, followed by drying over MgSO_4 . The crude **1** (1.46 g) was used in the next reaction. The analytical sample was purified with HPLC in chloroform. ^1H NMR ($\text{DMSO}-d_6$) δ 1.39 (s, 9H), 3.29 (s, 2H), 3.90 (s, 4H), 7.23 (m, 2H), 7.50 (m, 2H), 7.76 (m, 2H), 8.47 (m, 2H). ^{13}C NMR ($\text{DMSO}-d_6$) δ 27.7, 55.0, 59.1, 80.2, 122.1, 122.5, 136.4, 148.7, 158.9, 169.9. LRMS (NBA) [(M+H)⁺] calcd 314, found 314. HRMS (NBA) [(M+H)⁺] calcd 314.1863, found 314.1853.

2.3. Compound 2¹⁵

The crude **1** was refluxed in 1 N hydrochloric acid (55 mL) for 4 h, and after cooling to room temperature, the desired compound **2** was obtained as a white powder via the evaporation of the solvents (1.51 g, 4.10 mmol, 41%). ^1H NMR ($\text{DMSO}-d_6$) δ 3.64 (s, 2H), 4.47 (s, 4H), 7.88 (m, 2H), 8.05 (m, 2H), 8.44 (m, 2H), 8.78 (m, 2H). ^{13}C NMR ($\text{DMSO}-d_6$) δ 54.2, 54.8, 125.6, 126.4, 141.4, 145.5, 153.3, 171.5. LRMS (NBA) [(M+H)⁺] calcd. 258, found 258. HRMS (NBA) [(M+H)⁺] calcd. 258.1237, found 258.1235.

2.4. PMEAs

The compound **2** (0.916 g, 2.5 mmol) was dissolved in 20 mL of water and added triethylamine (1.04 mL, 7.5 mmol), *n*-propylamine (226 μL , 2.6 mmol), and DMT-MM (0.900 g, 3.25 mmol),

and the mixture was stirred at room temperature for 16 h. After the extraction with chloroform and washing with satd NaHCO_3 aq three times and brine, the organic layer was dried over MgSO_4 . After passing alumina chromatography in chloroform, the product was purified with HPLC in chloroform. After removing the solvent, the compound **3** was obtained as a white powder (100 mg, 0.335 mmol, 7%). ^1H NMR (D_2O) δ 0.59 (t, 3H, $J = 7.4$), 1.19 (m, 2H), 2.75 (t, 2H), 3.13 (s, 2H), 3.76 (s, 4H), 7.20 (m, 2H), 7.35 (m, 2H), 7.67 (m, 2H), 8.32 (m, 2H). ^{13}C NMR (D_2O) δ 11.2, 22.4, 41.3, 58.0, 61.6, 123.9, 125.2, 138.7, 148.9, 157.3, 173.9. LRMS (NBA) [(M+H)⁺] calcd 299, found 299. HRMS (NBA) [(M+H)⁺] calcd 299.1866, found 299.1860.

2.5. Octaammonium POSS 5

(3-Aminopropyl)triethoxysilane (100 mL, 0.427 mol) and concd hydrochloric acid (35–37%, 135 mL) in methanol (800 mL) produced **5** as a white precipitate after 5 days at room temperature. The product was obtained after filtration, washing with cold methanol, and drying. The compound **5** was spectroscopically pure in 30% yield (18.8 g). ^1H NMR ($\text{DMSO}-d_6$) δ 8.23 (s, 24H), 2.76 (t, 16H), 1.71 (m, 16H), 0.72 (t, 16H). ^{13}C NMR ($\text{DMSO}-d_6$) δ 40.53, 20.13, and 7.96. ^{29}Si NMR ($\text{DMSO}-d_6$) δ -66.4 (s). MALDI-TOF [(M+H)⁺] calcd 880.41, found 879.42.

2.6. F-POSS

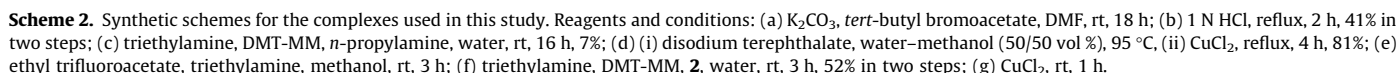
To a suspension of **5** (500 mg, 0.42 mmol) and ethyl trifluoroacetate (100 μL , 0.84 mmol) in methanol (20 mL), triethylamine (2 mL, 14.4 mmol) was added, and the reaction mixture was stirred at room temperature for 3 h. The resulting mixture was evaporated, and the crude product was directly used in the next step. The resulting product had, on average, 1.4 trifluoroacetyl groups according to ^1H NMR spectrum. ^1H NMR (D_2O) δ 3.26 (t, 2.8H, $J = 7.0$ Hz), 2.94 (t, 15.2H, $J = 7.0$ Hz), 1.70 (br s, 15.2H), 1.61 (br s, 2.8H), 0.64 (m, 16H); ^{13}C NMR (D_2O , 100 MHz) δ 155.9, 117.4, 41.52, 40.92, 21.76, 20.05, 8.77, 8.72; ^{29}Si NMR (D_2O) δ -68.4; ^{19}F NMR (D_2O) δ -75.4; MALDI-TOF [(M+H)⁺], [POSS-TFA₂] calcd 1074.52, found 1073.29, [POSS-TFA₃] calcd 1170.53, found 1170.00.

2.7. PMEAs-POSS

The reaction mixture containing F-POSS synthesized above, **2** (500 mg, 1.94 mmol), triethylamine (1 mL), and DMT-MM (800 mg) in methanol (30 mL) was stirred at room temperature for 3 h. After drying in vacuo and resolving the residue in methanol, 30 mL of acetonitrile containing 0.5 mL of hydrochloric acid was poured into the reaction solution, and then the supernatant was decanted. After resolving into methanol, the same procedure operation was executed twice. The product was obtained as a white powder after drying (333 mg, 0.22 mmol, 52%). The numbers of trifluoroacetyl, PMEAs, and ammonium groups were determined to be 1.4:1.4:5.2, respectively with the ^1H NMR measurements. The spectrum is shown below. ^1H NMR (CD_3OD) δ 0.64 (m, 5.6H), 0.75 (m, 10.4H), 1.65 (m, 5.6H), 1.80 (m, 10.4H), 2.92 (m, 10.4H), 3.13 (m, 2.8H), 3.64 (m, 2.8H), 3.99 (s, 2.8H), 4.41 (s, 5.6H), 7.83 (m, 2.8H), 7.93 (m, 2.8H), 8.37 (m, 2.8H), 8.78 (m, 2.8H). ^{29}Si NMR (CD_3OD) δ -66.0. ^{19}F NMR (D_2O) δ -75.4.

2.8. Complexation with Cu(II) ions

The standard sample of Cu-PMEAs was prepared according to the previous report¹⁵: The solution containing **3** (57.1 mg, 0.191 mmol) and disodium terephthalate (82 mg, 0.39 mmol) in a water-methanol (50 vol %) mixed solvent was heated at 95 °C



calcd 396, found 396. HRMS (NBA) [(M-Cl)⁺] calcd 396.0773, found 396.0760. Since same UV spectrum was observed from the aqueous sample containing **3** and CuCl₂ (1 equiv) without heating and according to the binding constant, we conclude that the

complexation should occur after mixing the ligand and CuCl_2 . Therefore, the complexation of PME-POSS with Cu(II) was executed only by mixing, and the products were used for further measurements.

2.9. UV titration for evaluating the binding affinities

The UV–vis spectrum of the Cu complexes (1 mM) was taken in 100 mM acetate buffers (pH 7.0) with a Shimadzu UV-3600 spectrophotometer using 1 cm path length cell at 25 °C. The binding constants of the complexes were calculated from the absorption at 705 nm of the solutions according to the equation below:

$$K_a = 10^{-3} \times (A_1 - A_{\text{obs}}) / (A_1 - A_0) / \{10^{-3} \times 1 - (A_1 - A_{\text{obs}}) / (A_1 - A_0)\}^2 \quad (1)$$

where A_1 is the absorption in the presence of an excess amount of Cu(II) , A_0 is the absorption of the chelators, and A_{obs} is the observed absorption value.

2.10. CV measurements

The current was measured in a three-electrode arrangement (ALS, model CV-50 W), a glassy carbon working electrode (electrode area, 3 mm²), a platinum counter electrode, and a sat. KCl reference electrode at 25 °C. The current measurements were performed with the Cu complex solutions (0.1 mM) in the presence or absence of GSH (1 mM) in 100 mM acetate (pH 7.0). CV conditions were 100 mV/min sweep speed, initial potential 0 V, and end potential +0.5 V.

2.11. Reduction of the Cu complexes

The samples containing each Cu complex (1 mM) in 100 mM acetate buffer (pH 7.0) were added to GSH or Angeli's salt and their spectra were immediately measured at 25 °C.

3. ¹⁹F NMR measurements for determining relaxation times

Relaxation times of the samples in ¹⁹F NMR were taken with the following parameter sets; relaxation delay, 15 s; pulse width (90°), 51 μs; acquisition time, 88 ms; scan time, 4 times. ¹⁹F longitudinal (T_1) relaxation data were collected with ten delay times (1, 5, 10, 20, 50, 100, 250, 500, 1000, and 3000 ms) using a standard 1D inverse recovery pulse sequence. ¹⁹F transverse (T_2) relaxation data were collected with nine delay times (400, 500, 600, 700, 800, 900, 1000, 2000, and 8000 ms) using a standard 1D Carr-Purcell-Meiboom-Gill pulse sequence. Resonance intensities in relaxation experiments were measured and fit to an exponential function. ¹⁹F NMR spectra for the analysis of synthetic compounds were taken at 25 °C with the following parameter sets; relaxation delay, 6 s; pulse width (45°), 12 μs; acquisition time, 88 ms; scan time, 8 times. Totally 1 min was required for 1D NMR acquisition.

4. Results and discussion

The chemical structures and synthetic protocols of the ¹⁹F NMR probe used in this study (Cu-POSS) and the model compound without the POSS moiety are shown in Scheme 2. The synthetic protocols are illustrated in Scheme 2. The probe is consisting of

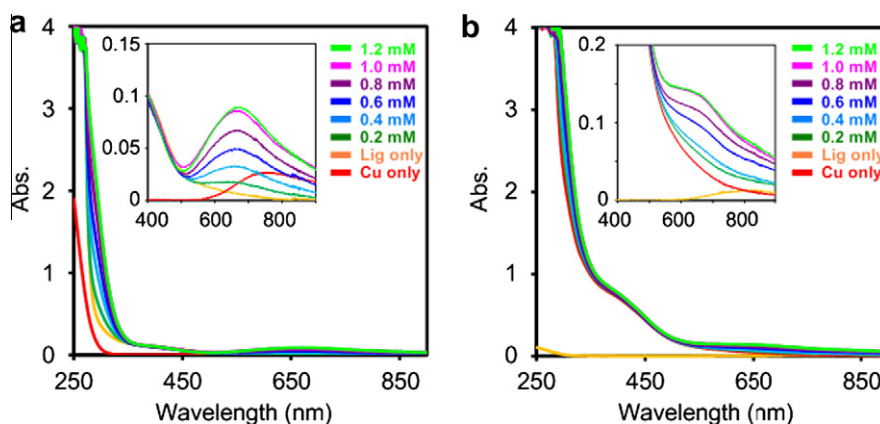


Figure 1. Absorption changes of 1 mM (a) PME and (b) PMEA-conjugated POSS by titrating CuCl_2 in 100 mM acetate buffer (pH 7.0) at 25 °C. The binding constants were estimated from the fitting curves plotted with the increases of the absorptions at 705 nm.

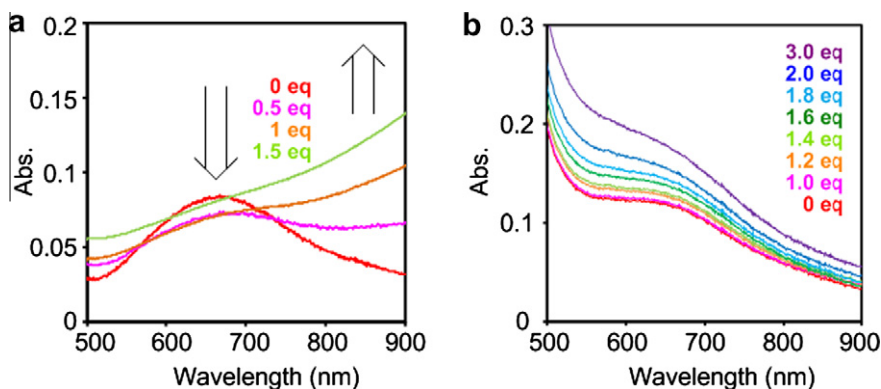


Figure 2. Absorption spectra of (a) 1 mM Cu-PMEA and (b) Cu-POSS with various concentrations of GSH in 100 mM acetate buffer (pH 7.0) at 25 °C.

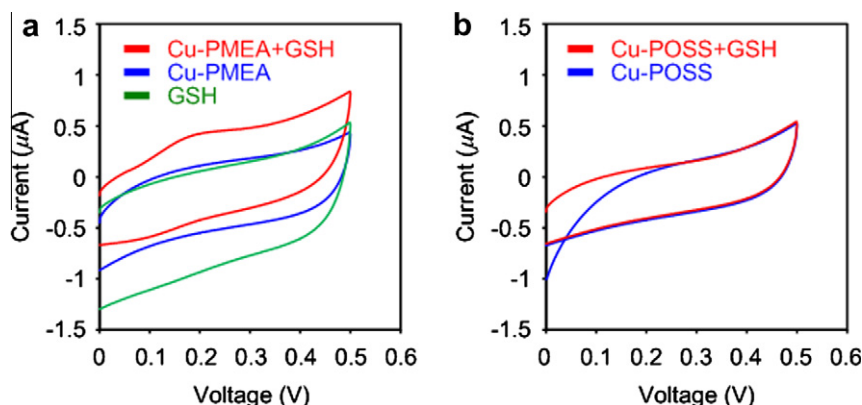


Figure 3. Cyclic voltammogram of the Cu complexes (0.1 mM) of (a) PMEA and (b) POSS with (red lines) or without (blue lines) adding 1 mM GSH.

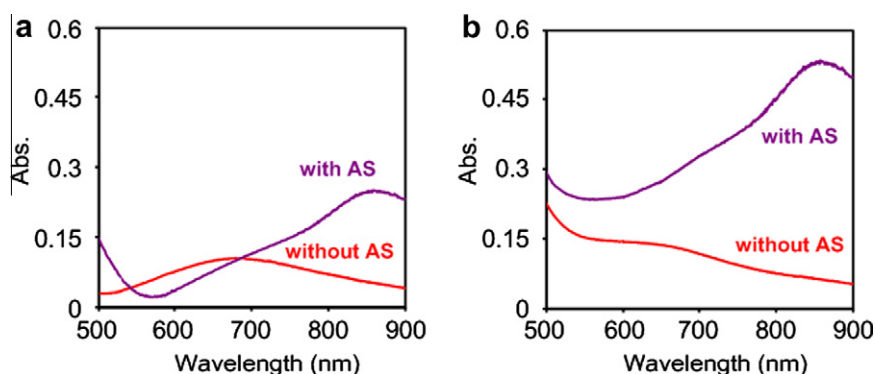


Figure 4. Absorption changes of 1 mM (a) Cu-PMEA and (b) Cu-POSS with or without Angeli's salt (2 mM) in 100 mM acetate buffer (pH 7.0) at 25 °C.

three parts, which are the Cu–PMEA complex for the signal modulation, trifluoroacetyl groups for the ^{19}F NMR signal, and aminoPOSS as a water-soluble scaffold for the assembly of functional molecules. Since the probe contains Cu(II) which displays paramagnetism, the relaxation should be strongly enhanced, leading to the increase of the peak width and the suppression of the signal intensities in the NMR spectra.^{10,14} By reducing Cu(II) to Cu(I) with HNO, the NMR signals of the probe should be recovered. Thereby, the existence of HNO can be monitored from the increase of the NMR signals. PRE strongly depends on a distance between paramagnetic species and observed nuclei,^{10,14,16} therefore compact structure of POSS (ca. 0.5 nm diameter) has an advantage to be used as a scaffold for presenting PRE efficiently.

The trifluoroacetyl groups and the PMEA ligands were tandemly introduced into octaaminoPOSS.¹⁷ The average numbers of fluorine atoms and the ligand in the single probe molecule were determined as 4.2 and 1.4 from the integration of ^1H NMR spectra, respectively. The products were purified as a water-soluble white powder from reprecipitation in acetonitrile containing 0.1% hydrochloric acid. Peak broadening in ^{19}F NMR spectra was not observed by adding to BSA (1 mg/mL) and the pH alteration between pH 5 and 9. These data indicate that undesired aggregation or non-specific adsorption of Cu–POSS could hardly occur in the measurements. These results suggest that the probes provide clear signal changes on the detection under biological conditions. We synthesized the propylamine-conjugated PMEA as a model compound without the POSS moiety.¹⁵ The fluorinated POSS without PMEA was also prepared to evaluate the effect of the covalently-tethering paramagnetic complex on signals.

To evaluate the complex stability, we estimated the binding constants of a Cu(II) ion to the ligand molecules. The titration

experiments were executed by monitoring UV–vis absorption corresponding to the d–d transition of a Cu(II) ion.¹⁸ The samples containing 1 mM of the ligands were added to the 100 mM acetate buffer solution (pH 7.0) containing 1 mM of CuCl_2 , and the absorption bands were monitored (Fig. 1). From the absorption changes at 705 nm, the binding constant of PMEA with a Cu(II) ion was determined as 51 mM^{-1} . We also measured the binding constant of the PMEA-conjugated POSS by the same procedure and calculated as 42 mM^{-1} . The result represents that the PMEA ligand can form stable complexes with a Cu(II) ion and the desorption of the chelated Cu ion from the complex could less occur under biological conditions. In addition, the POSS core hardly reduces the binding affinity of the ligand to a Cu(II) ion.

In order to evaluate the reactivity of the Cu(II) complexes with GSH, we carried out the titration experiments. The reduction of Cu(II) to Cu(I) was monitored by the decrease of the absorption band with the peak at 650 nm assigned as the d–d transition of Cu(II) and the increase of the absorption in the near infrared (NIR) region corresponded to the LMCT of Cu(I) (Fig. 2a).⁵ According to the increase of the amounts of GSH in the solutions, the

Table 1
NMR parameters of the fluorine atoms in POSS derivatives^a

Sample	T_1 (ms)	ΔT_1 (ms)	T_2 (ms)	ΔT_2 (ms)
F-POSS	1580	—	590	—
F-POSS+Cu–PMEA	1380	–200	460	–130
Cu–POSS	1180	–400	420	–170
Cu–POSS+GSH	1160	–420	410	–180
Cu–POSS+Angeli's salt	1460	–120	540	–50

^a Determined from the ^{19}F NMR measurements.

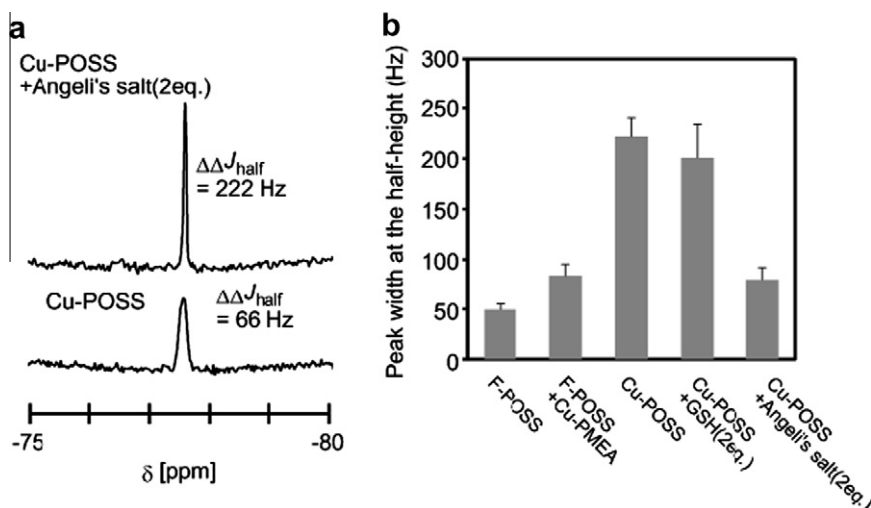


Figure 5. (a) ^{19}F NMR spectra of Cu-POSS (1 mM) with or without Angeli's salt (2 mM) in 100 mM acetate buffer (pH 7.0) at 25 °C. (b) The peak width at the half-height of ^{19}F NMR signals from the samples containing the POSS derivatives.

absorption band at 650 nm from Cu(II)–PMEA decreased, and the NIR absorption was enhanced. Subsequently, the absorption band reached a plateau by adding same equivalent of GSH. These data mean that the reduction of Cu(II)–PMEA to Cu(I)–PMEA can proceed quantitatively by adding GSH. Cyclic voltammogram of Cu(II)–PMEA (1 mM) showed the first oxidation peak of Cu(I) (+1.8 V) in the presence of 1 mM GSH (Fig. 3). From these results, it can be confirmed that the decreases of the absorption band with the peak at 650 nm should be caused from the reduction of Cu(II)–PMEA by adding GSH. Moreover, it is suggested that the dissociation of the Cu(II) ion from the chelator could hardly occur. In other words, it can be mentioned that the Cu(I) complex could be generated in the solution. Same experiments were carried out with Cu-POSS. Notably, significant increase of the absorption band was less observed (Fig. 2b). Furthermore, the reduction peak was not detected from the cyclic voltammograms (Fig. 3). These data clearly indicate that the reduction of Cu(II) should be crucially inhibited in Cu-POSS. The steric hindrance originated from POSS could reduce the accessibility of GSH to the Cu ion in the probe.

Next, the reactivities of the complexes to HNO were investigated. The UV–vis–NIR spectra were monitored before and after adding the Angeli's salt² (2 mM) which can generate HNO in water (Fig. 4). While to the distinct difference of the reactivity to GSH, both complexes gave similar changes in the spectra after adding the Angeli's salt. We observed the reduction of the absorption bands of the d–d transition at 650 nm and the increases of the LMCT bands at the NIR region. From these facts, it can be summarized that the Cu(II) ion in the POSS-tethered probes should be reduced not by GSH but by HNO. The samples containing Cu(II) complexes presented subtle changes in the absorption spectra after several days. On the other hand, after the storage of the sample containing the Cu(I) complexes for one day, the decreases of the absorption band in the NIR region were observed. The re-oxidation by the dissolved oxygen or two-electron reduction might occur.

We measured the longitudinal relaxation time (T_1) and the transverse relaxation time (T_2) of Cu-POSS in ^{19}F NMR before and after reduction (Table 1). By introducing the Cu(II) ion, the T_1 and T_2 decreased by 400 and 170 ms, respectively. The similar values of relaxation times of Cu-POSS were observed in the presence of 2 equiv of GSH. On the other hand, significant increases of both relaxation times were exhibited by 420 and 180 ms. From these results, it was confirmed that these acceleration of the relaxation times could be caused by PRE.

We evaluated the peak width of ^{19}F NMR of the complexes (1 mM) in 100 mM acetate buffer (pH 7.0) at 25 °C. The values of the peak width at the half-height are presented in Figure 5. In both cases of fluorinated POSS with or without the Cu-PMEA complex externally, the peak width was slightly influenced. In contrast, Cu-POSS showed the largest peak width of the samples. While the GSH addition less influenced the peak shapes, the significant increase of the peak width of ^{19}F NMR signals from Cu-POSS was observed by adding Angeli's salt to the solution ($\Delta\Delta_{\text{half}} = +156$ Hz). These results including the relaxation time measurements indicate that the Cu-PMEA complex covalently attached to POSS should be responsible for the signal regulation of ^{19}F NMR of the probe. The oxidation state corresponding to the magnetism of the Cu ions in the complexes dominates the ^{19}F NMR signals via PRE. Finally, although the GSH addition hardly influenced the NMR signals, the probe can show significant changes of ^{19}F NMR signals only in the presence of HNO.

5. Conclusion

We have presented here the synthesis of the ^{19}F NMR probes for detecting HNO. The Cu-POSS complexes showed high stability in the aqueous solutions. The oxidation states can be switched by reducing, resulting in the changes of ^{19}F NMR signals. Furthermore, because of the conjugation of the Cu complex with POSS, the probes have superior resistance to GSH. Our probes are promised to be feasible not only for imaging the distribution of HNO but also for monitoring the HNO behavior in the cells.

Acknowledgement

This research was partly supported by Shimadzu Science Foundation (for K.T.).

References and notes

- (a) Fukuto, J. M.; Carrington, S. J. *Antioxid. Redox Signal.* **2011**, *14*, 1649; (b) Kemp-Harper, B. K. *Antioxid. Redox Signal.* **2011**, *14*, 1609; (c) Bullen, M. L.; Miller, A. A.; Andrews, K. L.; Irvine, J. C.; Ritchie, R. H.; Sobey, C. G.; Kemp-Harper, B. K. *Antioxid. Redox Signal.* **2011**, *14*, 1675; (d) Irvine, J. C.; Ritchie, R. H.; Favalaro, J. L.; Andrews, K. L.; Widdop, R. E.; Kemp-Harper, B. K. *Trends Pharmacol. Sci.* **2008**, *29*, 601.
- Rosenthal, J.; Lippard, S. J. *J. Am. Chem. Soc.* **2010**, *132*, 5536.

3. (a) Zhou, Y.; Liu, K.; Li, J.-Y.; Fang, Y.; Zhao, T.-C.; Yao, C. *Org. Lett.* **2011**, *13*, 1290; (b) Choi, M. G.; Cha, S.; Lee, H.; Jeon, H. L.; Chang, S.-K. *Chem. Commun.* **2009**, 7390; (c) Xu, Z.; Han, S. J.; Lee, C.; Yoon, J.; Spring, D. R. *Chem. Commun.* **2010**, 46, 1679.
4. (a) Nordberg, J.; Arnér, E. S. J. *Free Radical Biol. Med.* **2001**, *31*, 1287; (b) Deneke, S. M.; Fanburg, B. L. *Am. J. Physiol.* **1989**, *257*, L163; (c) Carmel-Harel, O.; Storz, G. *Annu. Rev. Microbiol.* **2000**, *54*, 439.
5. Baek, H. K.; Holwerda, R. A. *Inorg. Chem.* **1983**, *22*, 3452.
6. (a) Tanaka, K.; Inafuku, K.; Chujo, Y. *Bioorg. Med. Chem.* **2008**, *16*, 10029; (b) Tanaka, K.; Kitamura, N.; Naka, K.; Chujo, Y. *Chem. Commun.* **2008**, 6176; (c) Tanaka, K.; Kitamura, N.; Chujo, Y. *Bioconjugate Chem.* **2011**, *22*, 1484.
7. (a) Tanaka, K.; Inafuku, K.; Naka, K.; Chujo, Y. *Org. Biomol. Chem.* **2008**, *6*, 3899; (b) Tanaka, K.; Inafuku, K.; Chujo, Y. *Chem. Commun.* **2010**, 46, 4378; (c) Tanaka, K.; Inafuku, K.; Adachi, S.; Chujo, Y. *Macromolecules* **2009**, *42*, 3489; (d) Tanaka, K.; Ohashi, W.; Kitamura, N.; Chujo, Y. *Bull. Chem. Soc. Jpn* **2011**, *84*, 612; (e) Tanaka, K.; Adachi, S.; Chujo, Y. *J. Polym. Sci. Part A: Polym. Chem.* **2009**, *47*, 5690; (f) Tanaka, K.; Adachi, S.; Chujo, Y. *J. Polym. Sci. Part A: Polym. Chem.* **2010**, *48*, 5712; (g) Tanaka, K.; Ishiguro, F.; Chujo, Y. *J. Am. Chem. Soc.* **2010**, *132*, 17649; (h) Tanaka, K.; Ishiguro, F.; Chujo, Y. *Polym. J.* **2011**, *43*, 708; (i) Tanaka, K.; Kitamura, N.; Naka, K.; Morita, M.; Inubushi, T.; Chujo, M.; Nagao, M.; Chujo, Y. *Polym. J.* **2009**, *41*, 287; (j) Tanaka, K.; Murakami, M.; Jeon, J.-H.; Chujo, Y. *Org. Biomol. Chem.* **2012**, *10*, 90; (k) Tanaka, K.; Chujo, Y. *J. Mater. Chem.* **2012**, *22*, 1733; (l) Tanaka, K.; Kitamura, N.; Chujo, Y. *Bioorg. Med. Chem.* **2012**, *20*, 96; (m) Tanaka, K.; Jeon, J.-H.; Inafuku, K.; Chujo, Y. *Bioorg. Med. Chem.* **2012**, *20*, 915.
8. Cui, W.; Otten, P.; Li, Y.; Koeneman, K. S.; Yu, J.; Mason, R. P. *Magn. Reson. Med.* **2004**, *51*, 616.
9. (a) Takaoka, Y.; Sakamoto, T.; Tsukiji, S.; Narazaki, M.; Matsuda, T.; Tochio, H.; Shirakawa, M.; Hamachi, I. *Nature Chem.* **2009**, *1*, 557; (b) Higuchi, M.; Iwata, N.; Matsuba, Y.; Sato, K.; Sasamoto, K.; Saido, T. C. *Nat. Neurosci.* **2005**, *8*, 527; (c) Doura, T.; An, Q.; Sugihara, F.; Matsuda, T.; Sando, S. *Chem. Lett.* **2011**, *40*, 1357; (d) Yamaguchi, K.; Ueki, R.; Nonaka, H.; Sugihara, F.; Matsuda, T.; Sando, S. *J. Am. Chem. Soc.* **2011**, *133*, 14208.
10. Mizukami, S.; Takikawa, R.; Sugihara, F.; Shirakawa, M.; Kikuchi, K. *Angew. Chem., Int. Ed.* **2009**, *48*, 3641.
11. (a) Oishi, M.; Sumitani, S.; Nagasaki, Y. *Bioconjug. Chem.* **2007**, *18*, 1379; (b) Kenwright, A. M.; Kuprov, I.; Luca, E. D.; Parker, D.; Pandya, S. U.; Senanayake, P. K.; Smith, D. G. *Chem. Commun.* **2008**, 2514; (c) Tanabe, K.; Harada, H.; Narazaki, M.; Tanaka, K.; Inafuku, K.; Komatsu, H.; Ito, T.; Yamada, H.; Chujo, Y.; Matsuda, T.; Hiraoka, M.; Nishimoto, S. *J. Am. Chem. Soc.* **2009**, *131*, 15982; (d) Langereis, S.; Keupp, J.; van Velthoven, J. L. J.; de Roos, I. H. C.; Burdinski, D.; Pikkemaat, J. A.; Grüll, H. J. *Am. Chem. Soc.* **2009**, *131*, 1380.
12. (a) Zimmermann, U.; Nöth, U.; Gröhn, P.; Jork, A.; Ulrichs, K.; Lutz, J.; Haase, A. *Artif. Cells Blood Substit. Immobil. Biotechnol.* **2000**, *28*, 129; (b) Ahrens, E. T.; Flores, R.; Xu, H. Y.; Morel, P. A. *Nat. Biotechnol.* **2005**, *23*, 983; (c) Maki, J.; Masuda, C.; Morikawa, S.; Morita, M.; Inubushi, T.; Matsusue, Y.; Taguchi, H.; Tooyama, I. *Biomaterials* **2007**, *28*, 434.
13. Tanaka, K.; Kitamura, N.; Takahashi, Y.; Chujo, Y. *Bioorg. Med. Chem.* **2009**, *17*, 3818.
14. Mizukami, S.; Takikawa, R.; Sugihara, F.; Hori, Y.; Tochio, H.; Wälchli, M.; Shirakawa, M.; Kikuchi, K. *J. Am. Chem. Soc.* **2008**, *130*, 794.
15. Choi, K.-Y.; Park, S.-Y.; Shin, A.-K. *J. Chem. Crystallogr.* **2006**, *36*, 7.
16. Sakamoto, T.; Shimizu, Y.; Sasaki, J.; Hayakawa, H.; Fujimoto, K. *Bioorg. Med. Chem. Lett.* **2011**, *21*, 303.
17. (a) Feher, F. J.; Wyndham, K. D. *Chem. Commun.* **1998**, 323; (b) Gravel, M.-C.; Zhang, C.; Dinderman, M.; Laine, R. M. *Appl. Organomet. Chem.* **1999**, *13*, 329.
18. Naka, K.; Fujita, M.; Tanaka, K.; Chujo, Y. *Langmuir* **2007**, *23*, 9057.